ARTICLE

Physicochemical and Electrochemical Properties of 1, 1, 2, 2-Tetrafluoroethyl-2, 2, 3, 3-Tetrafluoropropyl Ether as a Co-Solvent for High-Voltage Lithium-Ion Electrolytes

Lan Xia,[a] Saixi Lee,[b] Yabei Jiang,[b] Shiqi Li,[a] Zhaoping Liu,[b] Linpo Yu,[a] Di Hu,[a] and George Z. Chen*[a]

Abstract: Although high voltage positive materials for high energy density lithium-ion batteries have gained a great attention, the lack of compatible electrolytes with sufficiently high oxidative stability to deliver an excellent cycling ability restricts their practical application. Fluorinated solvents are considered as promising candidates for high-voltage electrolyte solvents. In this study, we select 1, 1, 2, 2-Tetrafluoroethyl-2, 2, 3, 3-tetrafluoropropyl ether (TTE) with high boiling point, low cost and good SEI-filming ability as a co-solvent of fluoroethylene carbonate-based electrolytes and extensively investigate its physicochemical and electrochemical properties for applications in high-voltage lithium-ion batteries. Our experimental results show that the TTE-containing electrolyte exhibits not only a high oxidative stability up to 5.5 V (*vs.* Li/Li^+), but also excellent wettability with the separator. In addition to high discharge capacity and increased coulombic efficiency of the $Li/LiNi_{0.5}Mn_{1.5}O_4$ half-cells assembled with the TTE-containing electrolyte cycled between 3.0 and 4.9 V, the cell also displays a high rate capability. This work shows that partially fluorinated ethers, e.g. TTE, are promising co-solvents for high-voltage electrolytes that can enable commercial development of high energy density lithium-ion batteries.

Introduction

Lithium-ion batteries (LIBs) have been envisioned as the most promising electrochemical energy storage devices for large-scale application in transportation and grid load levelling. Therefore, for this purpose, lithium-ion technology needs to be further improved with respect to energy and power density as well as long-term cycling stability and safety.[1] To increase the energy density, some new positive electrode materials are vigorously pursued. For instance, novel high capacity positive electrode materials, such as Li_2FeSiO_4 [2] and rich-Li Mn-based layered oxides $xLi_2MnO_3 \cdot (1-x)\ LiMO_2$ (M=Ni, Co, Mn) [3], and high-voltage positive electrode materials [4] with an operating voltage over 4.5 V, such as spinel-type $LiNi_{0.5}Mn_{1.5}O_4$ and olivine-type $LiMPO_4$ (M=Ni, Co, Mn), have been investigated extensively. Meanwhile, for nickel-rich layered oxides [5], $LiNi_{1-x-y}Co_xAl_yO_2$ and $LiNi_{1-x-y}Co_xMn_yO_2$ (x+y<0.2), a higher capacity can be delivered when charging to high voltages ≥4.5 V. However, a critical problem in using these positive electrode materials is capacity fading originated from ethylene carbonate (EC) oxidative decomposition at high operating potentials ≥4.5 V vs. Li/Li^+ [6]. Therefore, for practical applications of these novel positive electrode materials with high energy density, developing a stable and high-voltage electrolyte solvent still remains a priority.

In the literature, many efforts have been explored to address the unsatisfactory oxidation resistance of the conventional carbonate electrolytes, including introducing sacrificial additives to form a passivating layer on the surface of positive electrode [7], proposing superconcentrated electrolytes [8] and developing the intrinsic high-voltage stability of the electrolyte [9]. One of the most effective strategies to inhibit this issue is the development of novel stable solvents including ionic liquids, sulfones, dinitriles and fluorinated solvents for high-voltage electrolyte solutions [10]. Especially, because of the high electronegativity and low polarizability of the fluorine atom, fluorinated solvents are more difficult to oxidize electrochemically. Besides their higher oxidative stability, fluorinated solvents also deliver a higher flash point and lower melting point compared to the corresponding non-fluorinated solvents, and these properties can improve the safety and low-temperature performance, respectively [11]. Therefore, fluorinated solvents appear to be a suitable candidate for high-voltage electrolytes [12].

In previous studies, we had systematically investigated the oxidative decomposition mechanism of fluoroethylene carbonate (FEC) (EC was totally replaced by FEC) used in high-voltage batteries by DFT theoretical calculation and experimental comparison [13]. The result revealed that FEC-based electrolytes could offer excellent stability on the high-voltage positive electrode [13a]. However, the compatibility of these fluorinated electrolytes with graphite negative electrodes was found to be poor [13b]. To tackle this problem, we presented several methods, including negative electrode film-forming additives, namely lithium bis(oxalato)borate (LiBOB) and lithium difluoro(oxalato)borate (LiDFOB), and a new partially fluorinated ether co-solvent, 1,1,1,3,3,3-hexafluoroisopropyl methyl ether (HFPM), with the higher reduction potentials [13c]. The data demonstrated that these film-forming additives and co-solvents were beneficial for forming

[a] Dr. L. Xia, Dr. L.-P. Yu, Dr. D. Hu, S.-Q. Li, Prof. G.-Z. Chen
Department of Chemical and Environmental Engineering, Faculty of Science and Engineering
University of Nottingham Ningbo China
Taikang East Road 199, Ningbo 315100, China
E-mail: George.Chen@nottingham.edu.cn
[b] S. Lee, Y.-B. Jiang, Prof. Z.-P. Liu
Ningbo Institute of Materials Technology Engineering
Chinese Academy of Sciences (CAS)
Zhongguan West Road 1219, Ningbo 315201China

Supporting information for this article is given via a link at the end of the document.

WILEY-VCH

an effective SEI on the graphite negative electrode surface, resulting in enhanced stability in the negative side of high-voltage cell batteries. Especially, when adding some fluorinated ethers as co-solvents, the F-electrolyte displayed not only an excellent cycling stability in high-voltage batteries, but was also totally nonflammable in fire burning tests, which would be very useful for improving the battery safety [7a, 14]. However, we have also found that HFPM has some shortcomings such as extremely low boiling point of ~50°C, high volatility and high cost [15], which greatly limit further investigations and large scale applications. Thus, searching for more suitable fluorinated ethers with high boiling point, low cost as well as good compatibility with the graphite negative electrode is very much needed.

As early as in 2010, a partially fluorinated ether, 1, 1, 2, 2-tetrafluoroethyl-2, 2, 3, 3-tetrafluoropropyl ether (noted as TTE in the following text) was investigated for the first time as a co-solvent in LIBs with a $LiCoO_2$ positive electrode. The cell assembled with such fluorine-containing solvent (FCS)-based electrolytes displayed a high and stable discharge capacity in 30 cycles at a high upper cutoff voltage of 4.5 V [16]. However, the cell capacity still slowly decreased during the whole cycling period. Later, Nakajima et al. reported that addition of TTE in the electrolyte solution 0.67 mol L^{-1} $LiClO_4$/EC-DEC-PC (1:1:1 by volume) not only improved the thermal and electrochemical oxidation stability, but also increased the initial coulombic efficiencies due to the quick formation of SEI on graphite in this PC-containing solvents [17]. In recent years, many reports show that TTE can be widely used as a co-solvent in traditional ether-based electrolytes to suppress the polysulfide shuttle effect in lithium-sulfur batteries [18]. The reason is that the partially fluorinated ethers have multiple functions in battery electrolytes. Fluorinated ethers help to form mechanically stable SEI film on the surface of Li metal [18e, 18f], and they are also beneficial to forming a protection layer on the sulfur positive electrode through its reductive decomposition [19]. These results show that when TTE is added into the electrolytes, it is capable of improving the electrochemical oxidation stability of the proposed electrolytes, and helping to form a stable SEI on the surface of Li metal and graphite negative electrode. Furthermore, TTE has a higher boiling point of 93 °C and is widely used as a vapor decreasing solvent, a refrigerant, and an industrial cleaning agent [15, 20].

In this work, we aim to demonstrate TTE as a co-solvent for FEC-based electrolytes, and extensively investigate its physicochemical and electrochemical properties for applications in high-voltage LIBs. We firstly study the chemical stability of Li metal in pure TTE (as solvent) and the TTE-containing electrolyte. Additionally, the electrochemical performances of the pouch cells of artificial graphite/$LiNi_{1/3}Co_{1/3}Mn_{1/3}O_2$ with the TTE-containing electrolytes, and that with the base electrolyte are compared in terms of long-term cycling stability within the voltage range of 3.0-4.3 V at the rate of 1 C. The results demonstrate that as a prospective co-solvent, TTE with high boiling point and low cost displays not only good compatibility with graphite, but also superior cyclability at high voltages.

Results and Discussion

In order to clarify the solubility of lithium salt $LiPF_6$ in pure TTE solvent at room temperature, we measure 22.8 mg (calculated by 0.1 mol L^{-1}) and 1.5 mL TTE solvent respectively, then mix them for 1 day in an Ar-filled glovebox, and the result is showed in Figure 1b. From the picture of Figure 1b, we can see that the majority of lithium salt $LiPF_6$ is hardly insoluble in pure TTE solvent, which is attributed to its low donor ability [18b, 21]. Thus, its singer-solvent formulations cannot be prepared. For easy to compare with our previous work [13c], we prepare the TTE-containing electrolyte solution, which is 1 mol L^{-1} $LiPF_6$ in FEC/DMC/EMC/TTE 2:3:1:4 (by volume). Table 1 gives a comparison of the ionic conductivity, electrolyte uptake, and flammability of the TTE-containing electrolyte and the base electrolyte solution. The conductivity of the TTE-containing electrolyte is 6.50 mS cm^{-1}, which is lower than that of the base electrolyte (11.56 mS cm^{-1}). The reason is ascribed to the high viscosity of FEC and TTE.

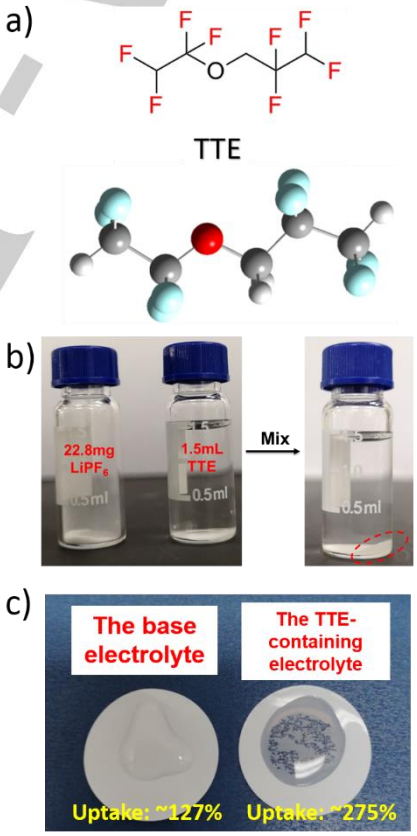

Figure 1. Chemical structure (a) of the TTE solvent, solubility (b) of lithium salt $LiPF_6$ in pure TTE solvent, and photograph of the wetting behavior (c) of the TTE electrolyte with the PP separator.

However, compared to the base electrolyte, the TTE-containing electrolyte has higher electrolyte uptake (275%) with separator. The better wettability behaviors of the TTE-containing electrolyte is further confirmed by adding a drop of the electrolytes to the surface of the separators, as displayed in Figure 1c.

Excellent wettability of the TTE-containing electrolyte with the separator will be beneficial for enhancing the power performances in battery operations. We all know that the use of high flammable organic electrolytes in current commercial lithium battery technology is a major cause for hazardous behaviors of lithium-ion batteries. Therefore, developing nonflammable electrolyte is very important for improving the safety of lithium-ion battery. As a comparison to the base electrolyte, the TTE-containing electrolyte is totally nonflammable (Table 1), which may stem from using fluorinated carbonate FEC and fluorinated ether TTE with no flash point.

Table 1. Summary of the basic characterizations of the TTE-containing electrolyte and the base electrolyte solution.

Electrolyte	Ionic conductivity / mS cm^{-1} [a]	Electrolyte uptake / %, with PP separator	Flammability / in fire
The base electrolyte	11.56	127	Inflammable
The TTE-Containing electrolyte	6.50	275	Nonflammable

[a] At 30°C.

To characterize the interactions between the solvents and the lithium salt of the TTE-containing electrolyte, Raman spectra of pure FEC, DMC, EMC, TTE, mixed solvent of FEC+DMC+EMC+TTE (2:3:1:4, by volume) and the TTE-containing electrolyte (1 mol L^{-1} $LiPF_6$/FEC + DMC + EMC + TTE (2:3:1:4, by volume)) are presented in Figure 2. For pure FEC, the C=O bending vibration and the C-C stretching vibration appears in the region ~730 and ~865 cm^{-1}. No changes are observed for these two peaks in the mixed solvents. However, when $LiPF_6$ is added in the mixed solvents, two new peaks appear at ~745 and ~870 cm^{-1}, respectively. These results are assigned to FEC molecules solvating lithium-ions. Meanwhile, the cis-cis vCH_3-O at 520 cm-1 and cis-trans vCH3-O at 920 cm-1 of DMC show similar trends. This would suggest that there is Li+-DMC coordination in the TTE-containing electrolyte. Besides, the C-F stretching vibration of TTE at 575~625 cm-1 in the mixed solvents has no obvious differences with the addition of the LiPF6, which may infer that there is no Li+-TTE coordination in the TTE-containing electrolyte.

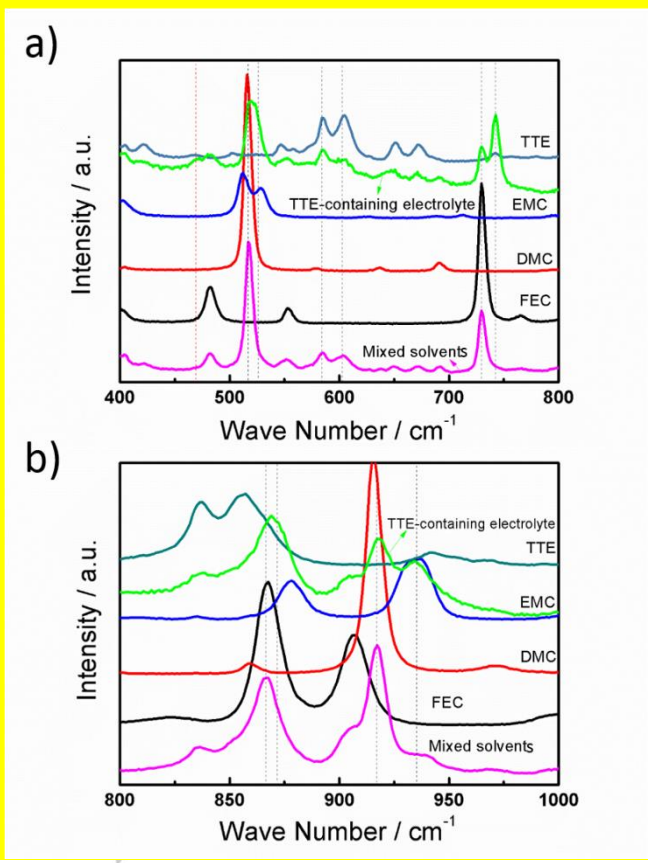

Figure 2. Raman spectra of pure FEC, DMC, EMC, TTE, mixed solvents of FEC+DMC+EMC+TTE (2:3:1:4, by volume) and the TTE-containing electrolyte (1 mol L^{-1} $LiPF_6$/FEC + DMC + EMC + TTE (2:3:1:4, by volume)). a) 400-800 cm^{-1}, a) 800-1000 cm^{-1}.

To evaluate the stability of lithium metal in the TTE pure solvent and the TTE-containing electrolyte solution, Figure 3 shows photographs of lithium metal in pure TTE solvent before and after storage in the Ar-filled glovebox at 25°C for 10 days. The surface of lithium sheet is scratched several times to expose bright lithium. From the left of photograph, the surface of Li sheet and its scratched areas are bright and no obvious change. In contrast, after storage for 10 days, the surface of Li sheet turns brownish black, its scratched areas have dimmed, and the color of the TTE solvent is no change after standing for 10 days. To clarify the surface morphology and composition of Li sheet stored in pure TTE solvent for 10 days, SEM images and EDX results, together with fresh Li sheet and Li sheet stored in TTE-containing electrolyte for comparison, are given in Figure 3 a-i and Table 2, respectively. Figure 3b, 3e and 3h show the scratched areas, and the Figure 3c, 3f and 3i display the other surface of Li sheet. As shown in Figure 3 a-c, the surface of fresh Li sheet is very compact. However, when Li sheet is stored in pure TTE solvent for 10 days, it can clearly be seen from the Figure 3e and 3f, the scratched area shows a layered network shape and the surface of Li sheet turn uneven, and its scratched area has a higher fluorine concentration as shown in Table 2.

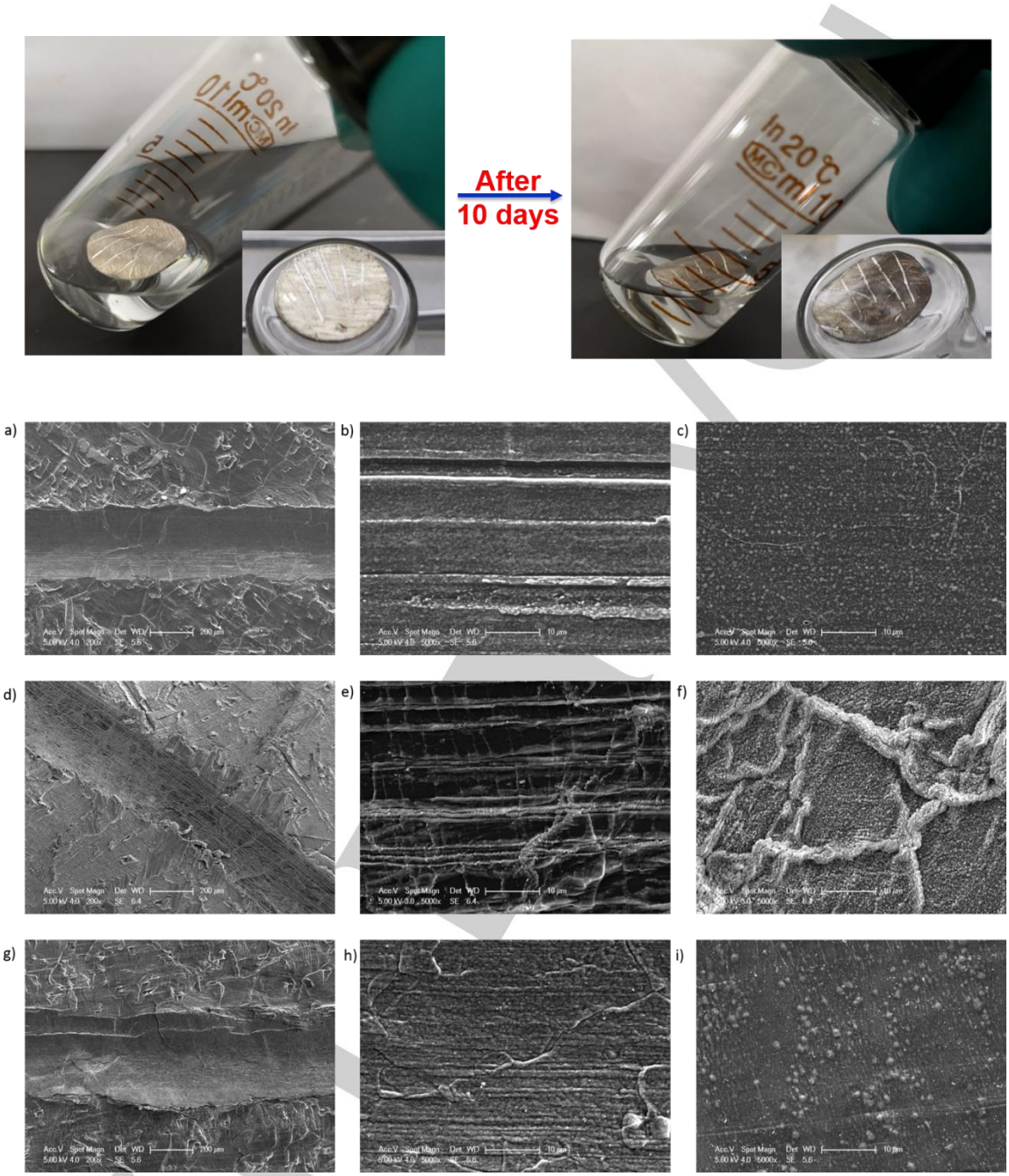

Figure 3. Photographs of lithium metal in pure TTE solvent before and after storage in the Ar-filled glovebox at 25ºC for 10 days; SEM images of fresh Li metal surface (a-c) and those being stored in pure TTE solvent (d-f) and the TTE-containing electrolyte solution (g-i) for 10 days.

The fluorine concentration represents the content of the fluorine-containing byproduct, which comes from the TTE solvent. These results means that TTE solvent slowly react with Li metal and can't form compact interfacial film on the surface of Li [22]. By contrast, for Li sheet stored in the TTE-containing electrolyte solution, as displayed in Figure 3 g-i, the scratched area on and surface of Li sheet is still compact, which infer that the Li sheet in the TTE-containing electrolyte can form an effective SEI film on its surface. Because the properties of the lithiated graphite electrode are similar to those of the Li metal, we indirectly deduce that the TTE-containing electrolyte is suitable for using in graphite-based negative electrodes.

Table 2. The composition (atomic %) of the scratched area on Li sheets after storage in the Ar-filled glovebox at 25°C for 10 days.

Electrolyte solution	EDX (Atomic %)		
	C	O	F
Fresh Li metal	16.21	83.79	---
The base electrolyte	3.50	87.17	9.33
The TTE-Containing electrolyte	4.07	89.97	6.16

To further clarify the surface component of the Li sheets being stored in pure TTE solvent and the TTE-containing electrolyte solution for 10 days, the C 1s and F 1s spectra were record, as seen in Figure 4. From the C 1s spectra of the Li sheet being stored in pure TTE solvent in the Figure 4a, there are C-F and C-O peaks, which indicate that the higher content of TTE reaction product with Li is deposited on the Li surface. In addition, as displayed in Figure 4b, the intensity of C-F and Li-F peaks at the surface of Li sheet stored in pure TTE solvent is higher than that in the TTE-containing electrolyte. These results reveal that TTE solvent is easy to react with Li metal, which is in accordance with the EDX results (Figure 3 and Table 2).

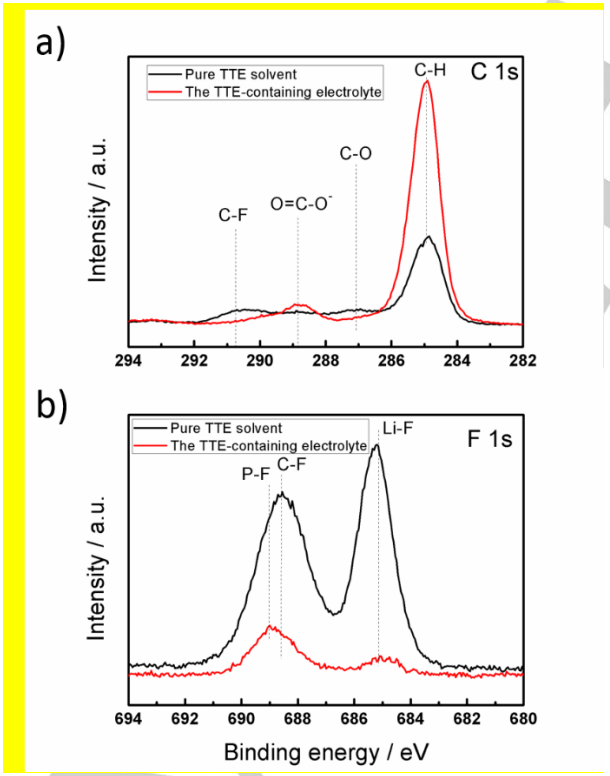

Figure 4. The C 1s and F 1s XPS spectra of the Li sheet being stored in pure TTE solvent and the TTE-containing electrolyte solution for 10 days.

Additionally, Figure S1 shows the cycling stability of the symmetric Li | Li cells with the base electrolyte and the TTE-containing electrolyte solution at a current density of 0.5 mA cm^{-2}. As presented in Figure S1, the voltage hysteresis of the cell in the TTE-containing electrolyte is about 0.1 V, and it remains relatively stable over 100 cycles. However, the cell with the base electrolyte shows gradually polarization phenomenon with increasing cycle number. This result displays that a relatively stable SEI layer can be formed when Li electrodes are cycled in the TTE-containing electrolyte.

To investigate the electrochemical window of the TTE-containing electrolyte, cyclic voltammetry (CV) measurements are performed. Figure 5 gives the CV curves of the base electrolyte (1mol L^{-1} $LiPF_6$/EC+DMC (3:7, by volume)) and the TTE-containing electrolyte solution (1 mol L^{-1} $LiPF_6$/FEC + DMC + EMC + TTE (2:3:1:4, by volume)) using a Pt microelectrode at a scan rate of 5 mV s^{-1}. As shown in Figure 5, we can find that the anodic current of the base electrolyte appears around 4.5 V vs. Li/Li^+, while the oxidation current for the TTE-containing electrolyte rises at an onset potential of 5.5 V, which is in accordance with the F-electrolyte solution reported in our previous results [13c]. The CV result indicates that the TTE-containing electrolyte shows high oxidation stability and can be used in high-voltage lithium-ion batteries.

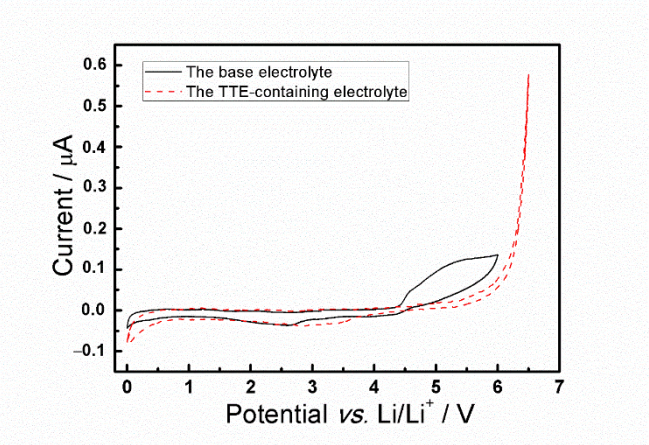

Figure 5. CV curves of the base electrolyte and the TTE-containing electrolyte solution using a Pt microelectrode at a scan rate of 5 mV s^{-1}.

Figure 6 gives comparisons of electrochemical properties of the $Li/LiNi_{0.5}Mn_{1.5}O_4$ half-cells cycled between 3.0 and 4.9 V at different rates using the base electrolyte and the TTE-containing electrolyte. As seen in Figure 6a, in the first cycle, the cell with the base electrolyte shows a slightly low discharge capacity of about 138 mAh g^{-1} and a relatively low coulombic efficiency of 73.7%, which may be due to its bad wettability with separator and its oxidation decomposition at high operating voltage. In contrast, with the TTE-containing electrolyte, the cell in the initial cycle displays a greatly higher reversible capacity of 147.7 mAh g^{-1} and demonstrates an obviously improved initial coulombic efficiency of 90.9%. Except for the high discharge capacity and increased

coulombic efficiency of the cell with the TTE-containing electrolyte, the cell also show a strong rate capability. As displayed in Figure 6b and Table S1, the cell with the TTE-containing electrolyte delivers reversible capacities of 148.4 mAh g^{-1} at 0.1 C, 147.5 mAh g^{-1} at the rate of 0.20 C, 140.7 mAh g^{-1} at the rate of 0.50 C and 138.6 mAh g^{-1} at the rate of 1.00 C. Even at 2.00 C, the cell can still deliver a high discharge capacity of 136.6 mAh g^{-1}. In contrast, the cell with the base electrolyte shows a low reversible capacity and a slightly poor rate capability. When the rate is returned to 1.00 C and the cell with these two electrolytes continue their charge-discharge behaviors. For the base electrolyte, the cell's capacity decreases to 127 mAh g^{-1} after 130 cycles, showing a low capacity retention of 94.8%. By contrast, the coin-cell assembled with the TTE-containing electrolyte displays a strong cyclability with a reversible capacity of 138 mAh g^{-1} at 200 cycle, corresponding to excellent capacity retention of 98.3% with respect to its highest capacity at 1.00 C, suggesting an enhancing the cycling stability and good rate capability of the TTE-containing electrolyte. Improving rate performance of the TTE-containing electrolyte may be attributed to its very good wettability with separator (see Figure 1c).

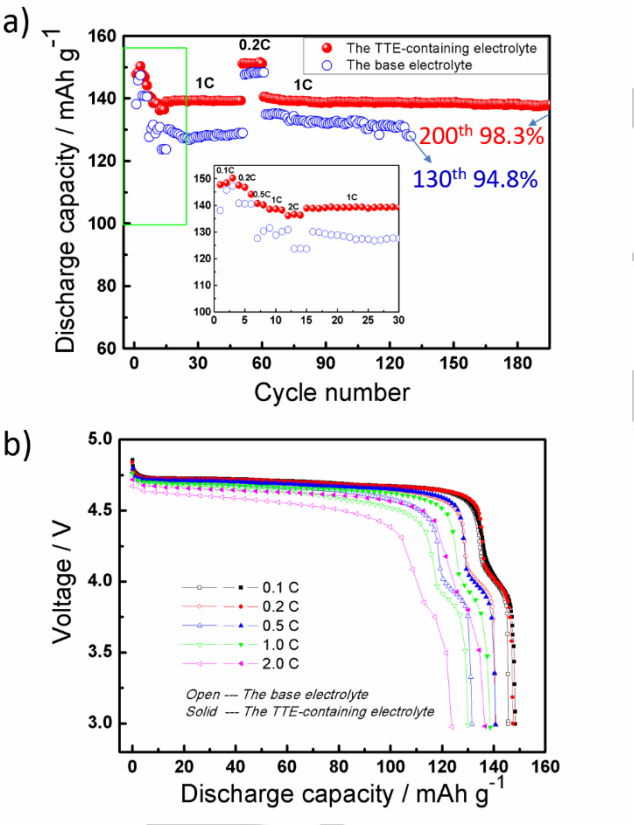

Figure 6. Electrochemical properties of the Li/$LiNi_{0.5}Mn_{1.5}O_4$ half-cells assembled with the base electrolyte and the TTE-containing electrolyte.

As we known, graphite-based negative electrodes are considered to be widely used in commercial lithium-ion batteries nowadays. Thus, it's very important to study the electrochemical stability of graphite electrodes in the TTE-containing electrolyte. Figure 7 gives the CV curves and discharge-charge curves of the Li/MCMB half-cells assembled with the TTE-containing electrolyte. Figure 7a shows the CV measurements of the Li/MCMB coin cells with the TTE-containing electrolyte at a scan rate of 0.1 mV s^{-1}, we can see that, in the 1st negative scan between 3.0 and 0 V, the MCMB electrode shows two weak reduction peaks around 1.5 and 1.0 V, which help to form the SEI film on the surface of MCMB electrode, and then these peaks disappear in subsequent scans. Meanwhile, there is a pair of redox peaks in the low operating voltage region from 0.50 to 0.01 V, showing a reversible lithium insertion/extraction reaction within the graphite layer. These CV results display that the TTE-containing electrolyte can form a stable SEI film on the surface of MCMB. We also can see from Figure 7b that the MCMB electrode delivers a high charge capacity of 379.4 mAh g^{-1} and a slightly high Coulombic efficiency of 85.5% in the first cycle and at 50 mA g^{-1}. In the first five cycles, the cell can still retain a high reversible capacity of 378 mAh g^{-1}. When the current density is increased to 100 mA g^{-1}, the galvanostatic discharge-charge curves for subsequent five cycles have no obvious change, and the charge capacity still has around 357 mAh g^{-1}, which further confirm a good cycling performance of the MCMB graphite electrode in the TTE-containing electrolyte. These data infer that the compatibility of the TTE-containing electrolyte used in the graphite negative electrode is good.

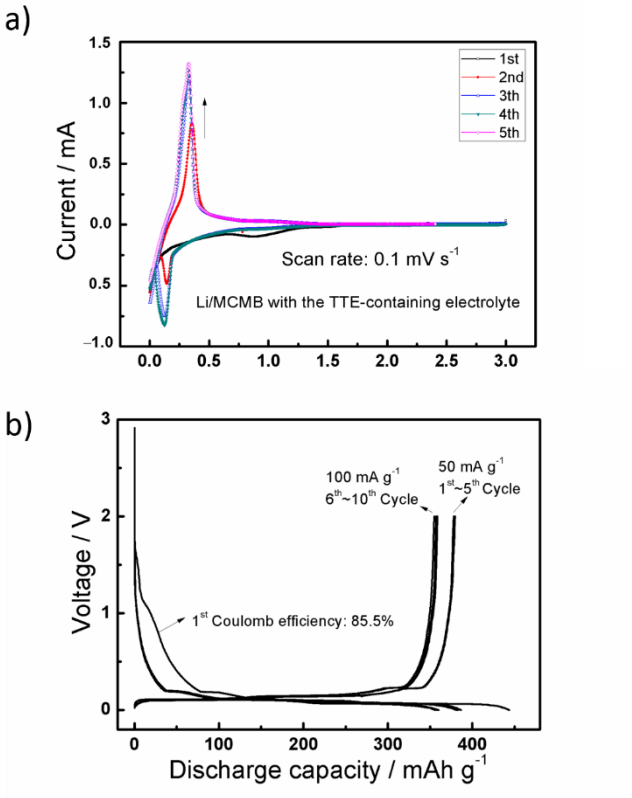

Figure 7. CV curves (a) and discharge-charge curves (b) of the Li/MCMB half-cells assembled with the TTE-containing electrolyte.

Figure 8 compares the electrochemical properties of high-voltage full 18650 batteries (MCMB/$LiNi_{0.5}Mn_{1.5}O_4$) with the TTE-containing electrolyte to those with the base electrolyte. As shown in Figure 8, in the initial cycle, the full batteries with these two electrolytes display very similar charge-discharge profiles and the same reversible capacity of 119 mAh g^{-1}. As the cycle number is increased from 1 to 35, the capacity retention of the 18650 battery in the base electrolyte decreases to 81% of its initial capacity, showing a poor cycling stability, which may be attributed to the oxidation decomposition of the electrolyte at the high operating voltage. In contrast, with the TTE-containing electrolyte, owing to its rather high anodic stability of, the battery after 35 cycles exhibits a highly reversible charge-discharge behavior with a high capacity retention of 93% of its first capacity. The result shows that the high-voltage full battery with the TTE-containing electrolyte has a better cycling stability than that with the base electrolyte.

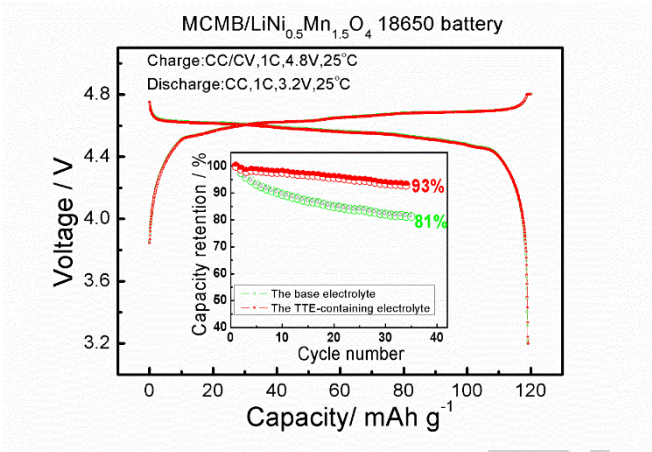

Figure 8. The electrochemical properties of the 18650 MCMB/$LiNi_{0.5}Mn_{1.5}O_4$ full-cells with the base electrolyte or the TTE-containing electrolyte within the voltage range from 3.2 to 4.8 V at the rate of 1.00 C.

To further investigate the properties of the TTE-containing electrolyte used in conventional lithium-ion batteries in practice, Figure 9 compares the electrochemical performance of the Artificial Graphite/$LiNi_{1/3}Co_{1/3}Mn_{1/3}O_2$ (AG/NMC111) pouch cells with the TTE-containing electrolyte to those with the base electrolyte. As shown in the Figure 9b, in the initial few cycles, the pouch cells with these two electrolytes at a cut-off voltage from 3.0 to 4.2 V, the cell shows a slightly higher discharge capacity in the TTE-containing electrolyte than in the base electrolyte. When the cut-off charge voltage is improved to 4.3 V, the reversible capacity of the cell assembled with the TTE-containing electrolyte increases to 1.137 Ah, which is higher than that of the cell with the base electrolyte (1.128 Ah). After 300 cycles, the discharge capacity of the pouch cell in the base electrolyte decrease to 1.084 Ah, and corresponding to capacity retention of 95.7%. In contrast, the cell with the TTE-containing electrolyte shows good cycling performance with a reversible capacity of 1.101 Ah at 300th cycle, and its capacity retention is 96.8%. Additionally, we can see from Figure 9c that the pouch cells with these two electrolytes demonstrate similar charge-discharge curves, while the cell shows a higher reversible capacity in the TTE-containing electrolyte than in the base electrolyte. These results suggest that the TTE-containing electrolyte can greatly enhance the electrochemical performances of the conventional pouch cells AG/NMC111, which may be due to the slightly lower interfacial resistance on the electrode surface and the higher oxidation stability. Our future work will further characterize the interfacial properties of the TTE-containing electrolyte on the CEI and SEI formation mechanism.

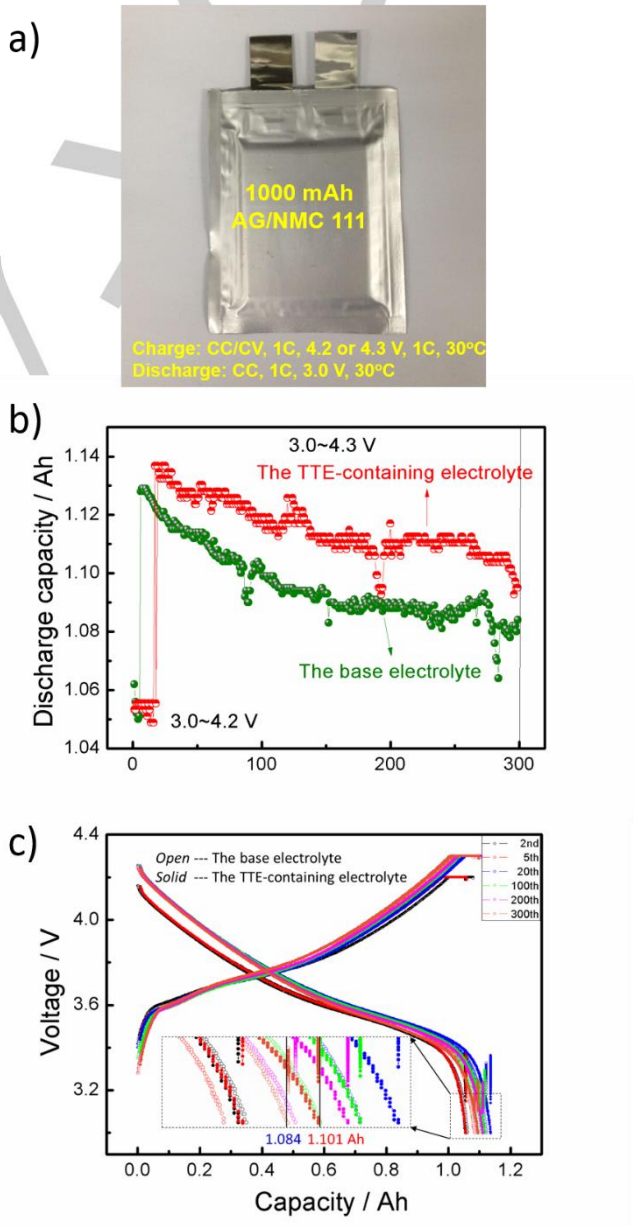

Figure 9. (a) Photograph of the 1000 mAh-Artificial Graphite/$LiNi_{1/3}Co_{1/3}Mn_{1/3}O_2$ (AG/NMC111) pouch cells, (b) capacity retention and (c) voltage profiles for the charge-discharge cycles according to the CC-CV protocol of the pouch cells within the voltage range of 3.0-4.3 V (or 4.2 V) at 1 C rate.

Conclusions

In summary, we have systematically studied the effects of adding the fluorinated ether-1, 1, 2, 2-Tetrafluoroethyl-2, 2, 3, 3-tetrafluoropropyl ether (TTE) with high anodic stability and good SEI-filming property as a co-solvent on the physicochemical properties of the FEC-based electrolyte and electrochemical performances of the high-voltage lithium-ion batteries. our results show that TTE solvent meets the demands for co-solvent of the FEC-based electrolytes, including good compatibility with graphite, favorable mobility, High boiling point and low cost, thus is suitable for cooperating with the FEC-based electrolyte to prepare high-voltage electrolytes. The cell using the TTE-containing electrolyte owns higher reversible capacity than the one with the base electrolyte, accompanied by quite stable cycle capability. Especially, the battery with the TTE-containing electrolyte exhibits the low polarization and excellent performance in the high-voltage measurement.

Experimental Section

1, 1, 2, 2-Tetrafluoroethyl-2, 2, 3, 3-tetrafluoropropyl ether (TTE, purity 98%) was purchased from J&K Scientific Ltd. without any additional in-house purification process. Li-battery-grade FEC, EC, DMC, EMC, and $LiPF_6$ was obtained from Suzhou Qianmin Chemical Reagent Co., Ltd. High-voltage spinel materials, $LiNi_{0.5}Mn_{1.5}O_4$ powder was kindly supplied by the Ningbo Institute of Materials Technology Engineering (NIMTE), Chinese Academy of Sciences (CAS). The $LiNi_{1/3}Co_{1/3}Mn_{1/3}O_2$ materials (The type is PLB-1) were purchased from ShenZhen Tianjiao Technology Co, Ltd. (ShenZhen, China). Li sheets (ϕ16mm*0.6mm, purity 99.9%) were purchased from China Energy Lithium Co., LTD. The base electrolyte solution used in this work was 1 mol L^{-1} $LiPF_6$ in EC/DMC 3:7 (by volume), and was purchased from Zhangjiagang Guotai Huarong New Chemical Materials Co. Ltd. The TTE-containing electrolyte was 1 mol L^{-1} $LiPF_6$ in FEC/DMC/EMC/TTE 2:3:1:4 (by volume), and prepared in an Ar-filled glovebox with an oxygen and H_2O level below 0.1 ppm. The coordination structure of the TTE-containing electrolyte was illustrated by inVia-Reflex Raman spectrometer (RENISHAW).

To see the solubility of lithium salt $LiPF_6$ in pure TTE solvent at room temperature, we mixed 22.8 mg (calculated by 0.1 mol L^{-1}) and 1.5 mL TTE solvent for 1 day in an Ar-filled glovebox. To study the stability of the Li sheet with pure TTE solvent and the TTE-containing electrolyte, Li sheets were immersed in pure TTE solvent and the TTE-containing electrolyte and then stored in an Ar glovebox for 10 days. Then, the Li sheets were collected with pure DMC washing to remove the precipitates and residual electrolytes on the Li sheet surface. Li sheet surface morphology was performed using field emission scanning electron microscopy (FESEM, Sirion 200, FEI, America). Meanwhile, the X-ray photoelectron spectroscopy (XPS) analyses were conducted using an AXIS Ultra DLD spectrometer with Al-Ka (1253.6 eV) radiation. The stored Li metal electrodes were rinsed with anhydrous DME three times (3 × 1 mL) to remove residual electrolyte salts and then dried in vacuum chamber. Rinsed Li metal electrodes were vacuum-sealed in an argon-filled glove box and then transferred to the XPS instrument for analysis.

The combustion behavior of the TTE-containing electrolyte by fire burning measurements was characterized [14b]. The ion conductivity of the TTE-containing electrolyte solution was measured on a DDS-307 equipment (INESA Scientific Instrument Co., Ltd, Shanghai, China) at 30°C. The wetting behaviors of the TTE-containing electrolytes are assessed by adding a drop of the electrolyte to the separator surface. Meanwhile, the electrolyte uptake (U) is obtained by determining the weight change of the separator before and after absorbing enough liquid electrolyte, which is calculated by the following equation:

$$U(\%) = \frac{M - M_0}{M_0} \times 100$$

Where M_0 and M represent the weight of the separator before and after absorbing enough liquid electrolyte, respectively. M_0 and M were measured for 3 times, then averaged the results.

Symmetric Li|Li cells were assembled by using Li metal as the working and counter electrodes. All the cells were charged and discharged at a current density of 0.5 mA cm^{-2}, and the cycling capacity was 1 mAh cm^{-2} for both charging and discharging processes.CV experiment of the TTE-containing electrolyte was conducted on a CHI660e electrochemical workstation (Chenhua Instrument Co., Shanghai, China) in a three-electrode electrochemical cell with a Pt disk as the working electrode and Li sheet as both reference and counter electrodes. The scan rate is 5 mV s^{-1}. To character the high-voltage battery performance with the TTE-containing electrolyte, CR2032-type coin half-cells of Li/$LiNi_{0.5}Mn_{1.5}O_4$ and Li/mesoporous carbon microbeads (MCMB) were investigated. The positive electrode is composed of 85 wt.% $LiNi_{0.5}Mn_{1.5}O_4$ active materials, 7 wt.% super P carbon black and 8 wt.% poly (Vinylidene fluoride) (PVDF), whereas the negative electrode consisted of 90 wt.% MCMB materials, 5 wt.% super P carbon black, and 5 wt.% PVDF. The separator is Celgard 2400 microporous membrane (Monolayer polypropylene (PP) separator). The CR2032-type coin cell is assembled in an Ar-filled glovebox. After assembly, the charge-discharge measurements were carried out on a Land CT2001A Battery Testing System (Wuhan, China).

The high-voltage MCMB/$LiNi_{0.5}Mn_{1.5}O_4$ 18650 batteries were built. The capacity of the batteries was 1500 mAh. The cylindrical batteries used polypropylene as the separator. The cycle performance tests of batteries with the base and TTE-containing electrolyte solution were tested by the software associated with LANDCT2001B battery test systems. Their electrochemical behaviors were performed at voltages from 3.2 to 4.8 V at 1500 mA (1.00 C) by using the constant-current constant-voltage (CC-CV) protocol. Additionally, we also used $LiNi_{1/3}Co_{1/3}Mn_{1/3}O_2$ as the positive electrode and built the artificial graphite/$LiNi_{1/3}Co_{1/3}Mn_{1/3}O_2$ pouch cells (1000 mAh, balanced for 4.2 V operation) without electrolyte. Artificial graphite used as the negative electrode active materials, and Celgard 2075 as the separator. Before electrolyte filling, the pouch cells were dried in a vacuum oven at 80°C for 12 h to remove any residual water. Then, the cells were transferred immediately into the Ar-filled glovebox, and a certain amount of electrolyte was poured into the cells and they were subsequent vacuum-sealed. The formation process and electrochemical behaviors of cells were tested by the software associated with LANDCT2001B battery test systems. For the formation process, the cells in this study were charged from OCV at 0.20 C to 4.2 V, held at 4.2 V to 0.02 C and then discharged to 3.0 V at 0.50 C. After the formation steps, the pouch cells were charged and discharged at 1.00 C between 3.0 and 4.2 V (or 4.3 V) with the constant-current constant-voltage (CC–CV) protocol. The cut-off current for CC-CV protocol was 0.05 C. The cycling tests were carried out at 30°C.

Acknowledgements

This research was financially supported by the National Natural Science Foundation of China under Grant No. 21503246, the

Ningbo Municipal Government (3315 Plan and the IAMET Special Fund, 2014A35001-1) and Zhejiang Provincial Natural Science Foundation of China under Grant No. LY19B030004.

Keywords: lithium-ion battery • high-voltage • solvent • fluorinated ether • 1, 1, 2, 2-tetrafluoroethyl-2, 2, 3, 3-tetrafluoropropyl ether

[1] a) B. Scrosati, J. Hassoun, Y.-K. Sun, *Energy Environ. Sci.* **2011**, *4*, 3287−3295; b) M. M. Thackeray, C. Wolverton, E. D. Isaacs, *Energy Environ. Sci.* **2012**, *5*, 7854−7863; c) M. Winter, B. Barnett, K. Xu, *Chem. Rev.* **2018**, *118*, 11433-11456; d) Q. Wang, L. Jiang, Y. Yu, J. Sun, *Nano Energy* **2019**, *55*, 93-114.

[2] a) A. Manthiram, *J. Phys. Chem. Lett.* **2011**, *2*, 176-184; b) M. Hu, X. Pang, Z. Zhou, *J. Power Sources* **2013**, *237*, 229-242.

[3] a) P. Rozier, J. M. Tarascon, *J. Electrochem. Soc.* **2015**, *162*, A2490-A2499; b) E.M. Erickson, F. Schipper, T.R. Penki, J.-Y. Shin, C. Erk, F.-F. Chesneau, B. Markovsky, D. Aurbach, *J. Electrochem. Soc.* **2017**, *164*, A6341-A6348.

[4] a) A. Manthiram, K. Chemelewski, E.-S. Lee, *Energy Environ. Sci.* **2014**, *7*, 1339-1350; b) X. Zhang, F. Cheng, J. Yang, J. Chen, *Nano Lett.* **2013**, *13*, 2822–2825; c) W. Sun, Y. Li, K. Xie, S. Luo, G. Bai, X. Tan, C. Zheng, *Nano Energy* **2018**, *54*, 175-183.

[5] a) J.-c. Zheng, Z. Yang, Z.-j. He, H. Tong, W.-j. Yu, J.-f. Zhang, *Nano Energy* **2018**, *53*, 613-621; b) A. Manthiram, J.C. Knight, S.-T. Myung, S.-M. Oh, Y.-K. Sun, *Adv. Energy Mater.* **2016**, *6*, 1501010; c) F. Schipper, E.M. Erickson, C. Erk, J.-Y. Shin, F.F. Chesneau, D. Aurbach, *J. Electrochem. Soc.* **2017**, *164*, A6220-A6228.

[6] a) M. Egashira, H. Takahashi, S. Okada, J.-i. Yamaki, *J. Power Sources* **2001**, *92*, 267–271; b) M. A. Teshager, S. D. Lin, B.-J. Hwang, F.-M. Wang, S. Hy, A. M. Haregewoin, *ChemElectroChem* **2016**, *3(2)*, 337-345.

[7] a) C.-K. Kim, D.-S. Shin, K.-E. Kim, K. Shin, J.-J. Woo, S. Kim, S. Y. Hong, N.-S. Choi, *ChemElectroChem* **2016**, *3(6)*, 913-921; b) J.-G. Han, J. B. Lee, A. Cha, T. K. Lee, W. Cho, S. Chae, S. J. Kang, S. K. Kwak, J. Cho, S. Y. Hong, N.-S. Choi, *Energy Environ. Sci.* **2018**, *11*, 1552-1562; c) L. Wang, Y. Ma, Q. Li, Z. Zhou, X. Cheng, P. Zuo, C. Du, Y. Gao, G. Yin, *J. Power Sources* **2017**, *361*, 227-236.

[8] a) J. Wang, Y. Yamada, K. Sodeyama, C. H. Chiang, Y. Tateyama, A. Yamada, *Nat. Commun.* **2016**, *7*, 12032; b) L. Xia, L. Yu, D. Hu, G.Z. Chen, *Mater. Chem. Front.* **2017**, *1*, 584-618.

[9] A. Tornheim, S. Sharifi-Asl, J. C. Garcia, J. Bareño, H. Iddir, R. Shahbazian-Yassar, Z. Zhang, *Nano Energy* **2019**, *55*, 216-225.

[10] a) D. M. Poper, T. Evans, K. Leung, T. Watkins, J. Olson, S. C. Kim, S. S. Han, V. Bhat, K. H. Oh, D. A. Buttry, S.-H. Lee, *Nat. Commun.* **2015**, *6*, 7230-7239; b) M. Kerner, D.-H. Lim, S. Jeschke, T. Rydholm, J.-H. Ahn, J. Scheers, *J. Power Sources* **2016**, *332*, 204–212; c) B. Flamme, M. Haddad, P. Phansavath, V. Ratovelomanana-Vidal, A. Chagnes, *ChemElectroChem* **2018**, *5(16)*, 2279-2287; d) C.-C. Su, M. He, P. Redfern, L. A. Curtiss, C. Liao, L. Zhang, A. K. Burrell, Z. Zhang, *ChemElectroChem*, **2016**, *3*, 790–797; e) C.-C. Su, M. He, P. C. Redfern, L. A.Curtiss, I. A. Shkrob, Z. Zhang, *Energy Environ. Sci.* **2017**, *10*, 900-904.

[11] a) N. Nanbu, M. Takehara, S. Watanabe, M. Ue, Y. Sasaki, *Bull. Chem. Soc. Jpn.* **2007**, *80*, 1302−1306; b) T. Achiha, T. Nakajima, Y. Ohzawa, M. Koh, A. Yamauchi, M. Kagawa, H. Aoyama, *J. Electrochem. Soc.* **2009**, *156*, A483−A488.

[12] a) Z. Zhang, L. Hu, H. Wu, W. Weng, M. Koh, P.C. Redfern, L.A. Curtiss, K. Amine, *Energy Environ. Sci.* **2013**, *6*, 1806–1810; b) M. Bolloli, J. Kalhoff, F. Alloin, D. Bresser, Le, M.L. Phung, B. Langlois, S. Passerini, J.-Y. Sanchez, *J. Phys. Chem. C* **2015**, *119*, 22404–22414; c) M. He, L. Hu, Z. Xue, C.C. Su, P. Redfern, L.A. Curtiss, B. Polzin, A.v. Cresce, K. Xu, Z. Zhang, *J. Electrochem. Soc.* **2015**, *162*, A1725–A1729; d) L. Hu, K. Amine, Z. Zhang, *Electrochem. Commun.* **2014**, *44*, 34–37; e) L. Hu, Z. Zhang, K. Amine, *Electrochem. Commun.* **2013**, *35*, 76–79; f) J. Xia, M. Nie, J.C. Burns, A. Xiao, W.M. Lamanna, J. R. Dahn, *J. Power Sources* **2016**, *307*, 340-350.

[13] a) L. Xia, B. Tang, L. Yao, K. Wang, A. Cheris, Y. Pan, S. Lee, Y. Xia, G.Z. Chen, Z. Liu, *ChemistrySelect* **2017**, *2*, 7353-7361; b) L. Xia, S. Lee, Y. Jiang, Y. Xia, G. Z. Chen, Z. Liu, *ACS Omega* **2017**, *2*, 8741-8750; c) L. Xia, Y.-G. Xia, C. Wang, H. Hu, S. Lee, Q. Yu, H. Chen, Z.-P. Liu, *ChemElectroChem* **2015**, *2*, 1707-1712.

[14] a) L. Xia, L. Yu, D. Hu, G. Z. Chen, *Acta Chim. Sinica* **2017**, *75*, 1183–1195; b) L. Xia, Y.-G. Xia, Z.-P. Liu, *J. Power Sources* **2015**, *278*, 190-196.

[15] a) J. Murata, S. Yamashita, M. Akiyama, S. Katayama, T. Hiaki, A. Sekiya, *J. Chem. Eng. Data* **2002**, *47*, 911−915; b) M. Yasumoto, Y. Yamada, J. Murata, S. Urata, K. Otake, *J. Chem. Eng. Data* **2003**, *48*, 1368−1379.

[16] a) T. Kitagawa, K. Azuma, M. Koh, A. Yamauchi, M. Kagawa, H. Sakata, H. Miyawaki, A. Nakazono, H. Arima, M. Yamagata, M. Ishikawa, *Electrochemistry* **2010**, *78*, 345-348; b) M. Ishikawa, M. Yamagata, T. Sugimoto, Y. Atsumi, T. Kitagawa, K. Azuma, *ECS Trans.* **2011**, *33*, 29-36.

[17] a) T. Achiha, T. Nakajima, Y. Ohzawa, M. Koh, A. Yamauchi, M. Kagawa, H. Aoyama, *J. Electrochem. Soc.* **2010**, *157*, A707-A712; b) N. Ohmi, T. Nakajima, Y. Ohzawa, M. Koh, A. Yamauchi, M. Kagawa, H. Aoyama, *J. Power Sources* **2013**, *221*, 6-13.

[18] a) N. Azimi, W. Weng, C. Takoudis, Z. Zhang, *Electrochem. Commun.* **2013**, *37*, 96-99; b) H. Lu, Y. Yuan, Z. Hou, Y. Lai, K. Zhang, Y. Liu, *RSC Advances* **2016**, *6*, 18186-18190; c) S. Gu, R. Qian, J. Jin, Q. Wang, J. Guo, S. Zhang, S. Zhuo, Z. Wen, *Phys. Chem. Chem. Phys.* **2016**, 18, 29293-29299; d) C. Zu, N. Azimi, Z. Zhang, A. Manthiram, *J. Mater. Chem. A* **2015**, *3*, 14864-14870; e) H. Lu, Y. Yuan, K. Zhang, F. Qin, Y. Lai, Y. Liu, *J. Electrochem. Soc.* **2015**, *162*, A1460-A1465.

[19] a) N. Azimi, Z. Xue, N. D. Rago, C. Takoudis, M. L. Gordin, J. Song, D. Wang, Z. Zhang, *J. Electrochem. Soc.* **2015**, *162*, A64-A68; b) N. Azimi, Z. Xue, I. Bloom, M. L. Gordin, D. Wang, T. Daniel, C. Takoudis, Z. Zhang, *ACS Appl. Mater. Interfaces* **2015**, *7*, 9169-9177.

[20] a) P. Blowers, D. M. Moline, K. F. Tetrault, R. R. Wheeler, S. L. Tuchawena, *Environ. Sci. Technol.* **2008**, *42*, 1301−1307; b) A. Foris, *Magn. Reson. Chem.* **2004**, *42*, 534−555; c) S. Ando, *J. Photopolym. Sci. Technol.* **2006**, *19*, 351−360.

[21] M. Cuisinier, P.E. Cabelguen, B.D. Adams, A. Garsuch, M. Balasubramanian, L.F. Nazar, *Energy Environ. Sci.* **2014**, *7*, 2697–2705.

[22] L. Kavan, *Chem. Rev.* **1997**, *97*, 3061-3082.

ARTICLE

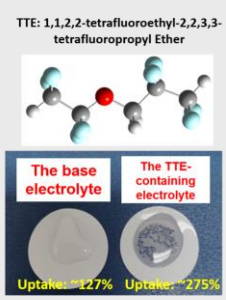

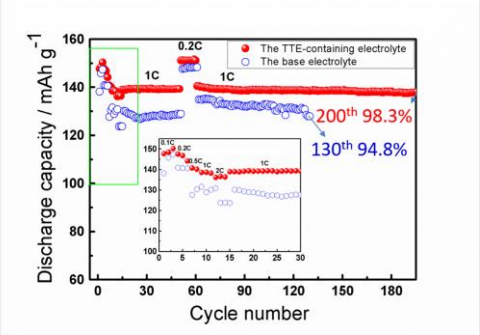

1, 1, 2, 2-Tetrafluoroethyl-2, 2, 3, 3-tetrafluoropropyl ether (TTE) is of high boiling point, low cost and good SEI-filming ability and has been selected as a co-solvent of the fluoroethylene carbonate-based electrolytes. In addition to the high discharge capacity and increased coulombic efficiency of the Li/$LiNi_{0.5}Mn_{1.5}O_4$ half-cell assembled with the TTE-containing electrolyte cycled between 3.0 and 4.9 V, the cell also displays a notably higher rate capability. This work indicates that fluorinated ethers, such as TTE, may be a prospective co-solvent for high-voltage electrolytes enabling commercially desirable high energy density lithium-ion batteries.

*L. Xia, S. Lee, Y. Jiang, S. Li, Z. Liu, L. Yu, D. Hu, G. Z. Chen**

Page No. – Page No.

Physicochemical and Electrochemical Properties of 1, 1, 2, 2-Tetrafluoroethyl-2, 2, 3, 3-Tetrafluoropropyl Ether as a Co-Solvent for High-Voltage Lithium-Ion Electrolytes

WILEY-VCH